GEOSCIENCE CANADA
JOURNAL OF THE GEOLOGICAL ASSOCIATION OF CANADA
JOURNAL DE L'ASSOCIATION GÉOLOGIQUE DU CANADA

IN PRESS ARTICLE

Remote Predictive Mapping 5. Using a Lidar Derived DEM to Test the Influence of Variable Overburden Thickness and Bedrock on Drainage and Basin Morphology

Tim L. Webster, John C. Gosse, Ian Spooner, and J. Brendan Murphy

DOI: http://www.dx.doi.org/10.12789/geocanj.2014.41.033

To appear in: Geoscience Canada

Received: April 2012
Accepted as revised: July 2013
First published on the web: January 2014

SERIES

Remote Predictive Mapping 5. Using a Lidar Derived DEM to Test the Influence of Variable Overburden Thickness and Bedrock on Drainage and Basin Morphology

Tim L. Webster[1], John C. Gosse[2], Ian Spooner[3], and J. Brendan Murphy[4]

[1]Applied Geomatics Research Group
Nova Scotia Community College
50 Elliot Rd. Lawrencetown, NS, Canada, B0S 1M0
Email, tim.webster@nscc.ca

[2]Department of Earth Sciences
Dalhousie University
Edzell Castle Circle
Halifax, NS, Canada, B3H 4R2

[3]Geology Department
Acadia University
Wolfville, NS, Canada, B4P 2R6

[4]Department of Earth Sciences
Saint Francis Xavier University
Antigonish, Nova Scotia, B2G 2W5

SUMMARY

A 4–m lidar digital elevation model (DEM) provides sufficient resolution to examine the impact of variable till cover on the incision history of multiple small (5 km^2) catchments in eastern Canada. The study site was selected because it has homogeneous bedrock geology that dips parallel to the land surface, is tectonically stable, has undergone common base level changes, and has a common ice history, with variable overburden thickness, from thin cover in the west to thick cover in the east. Basin morphometrics were compared for similar-size basins that have variable till cover thicknesses. Basins with thicker till cover are wider and show differences in hypsometries compared to those where till cover is thin. Two basins representing end members of till thickness were measured for stream discharge and water chemistry. Thick till (> 1 m) on the eastern half of North Mountain retards infiltration sufficiently to promote overland flow and accelerate incision relative to areas with thinner till. Till thickness and continuity therefore are expected to impede the achievement of steadiness and may also delay stream power law relationships in larger catchments until till cover has been effectively eroded.

SOMMAIRE

Un modèle altimétrique numérique (MAN) par lidar 4 m offre une résolution suffisante pour étudier l'impact des divers dépôts de till sur l'histoire de l'érosion linéaire de multiples petits (5 km^2) bassins versants dans l'Est du Canada. Le site d'étude a été choisi parce que sa géologie est homogène et que son pendage est parallèle à la surface du sol, qu'il est tectoniquement stable, qu'il a subi des changements similaires du niveau de base d'érosion, de même qu' une histoire glaciaire similaire, avec une épaisseur de mort-terrain variable, d'une couverture mince à l'ouest jusqu'à une couverture épaisse à l'est. La morphométrie du bassin a été comparée à celle de bassins de taille semblable aux épaisseurs de till variables. Les bassins aux couvertures de till plus épaisses sont plus larges et montrent des différences hypsométriques comparé à ceux aux couvertures minces. Deux bassins représentant les termes extrêmes de l'épaisseur du till ont été mesurées quant au débit du courant et à la chimie de l'eau. Les till épais (>1 m) sur la moitié est du mont Nord retardent l'infiltration, ce qui favorise l'écoulement en surface et accélèrent l'érosion linéaire par rapport aux zones couvertes de couches de till plus minces. On s'attend donc à ce que l'épaisseur de la couche de till et sa continuité agissent comme une entrave à la stabilité et puissent aussi retarder les effets de la loi de puissance de l'écoulement dans les grands bassins récepteurs jusqu'à ce que la couverture de till a été effectivement érodée.

INTRODUCTION

Understanding the relationships between stream incision and factors related to fluvial erosion such as rock-uplift, climate, base level changes, and bedrock resistance to erosion (e.g. Seidl

et al. 1994; Gíslason et al. 1996; Stock and Montgomery 1999; Kirby and Whipple 2001; Stock et al. 2005) is important for the analysis of landscape evolution (e.g. Pazzaglia 1993, 2003; Kooi and Beaumont 1996; Dietrich et al. 2003). The mechanics of river incision have been studied by Whipple et al. (2000), Whipple and Tucker (2002) and related to rock strength by Sklar and Dietrich (2001). The availability of high resolution (4 m) Light Detection and Ranging (lidar) DEMs can facilitate quantitative analysis of incision and basin morphometrics at sufficiently small scales to allow the examination of factors controlling stream evolution. Fluvial processes in glaciated terrain are complex because glaciers and streams may sequentially occupy the same valleys but each can uniquely contribute to erosion, making the relative influence of glacial and fluvial processes on valley size difficult to distinguish. In addition to glacial processes shaping the landscape glacial till deposits can influence the permeability of basin sediments and can affect drainage characteristics, such as over land flow and infiltration of precipitation. Brocklehurst and Whipple (2002, 2004) and Montgomery (2002) use morphometric analysis including hypsometry and valley cross-sections to differentiate large catchments affected by alpine glacial processes from others that were affected only by fluvial processes. They concluded that although glaciers widen and deepen valleys, significant relief enhancements are limited to large alpine glaciers. Studies applying the stream power law often use the contributing drainage area as a surrogate parameter for stream discharge, which in addition to the local channel slope, controls the stream's ability to incise the underlying bed (e.g. Stock and Montgomery 1999; Snyder et al. 2000):

$$E = KA^m S^n \quad (Eq.\ 1)$$

Where E is the erosion rate, K represents the bedrock erodibility factor, A is the contributing drainage area, and S is the channel slope. The exponents m and n are typically derived empirically. Few studies, however, examine the local hydrological effects of surface materials, such as glacial till cover, and groundwater interaction on discharge (Tague and Grant 2004). At the scale of basin areas of tens of square kilometres and larger, factors such as overburden thickness and the fracture density of bedrock can strongly influence infiltration rates and affect peak annual stream discharge.

Although the effect of DEM resolution on measuring different hydrologic and geomorphic properties has been examined (e.g. Wolock and Price 1994; Zhang and Montgomery 1994; Gao 1997; Zang et al. 1999; Walker and Willgoose 1999), most of these studies have focused on the different effects of grid cell size interpolated from similar source data from photogrammetry rather than advances in data acquisition technologies such as laser altimetry. In this study, the high-resolution of the lidar (Light Detection and Ranging) DEM allows detailed analysis of basin morphometrics to assess the local effects of variable overburden thickness within a region. Lidar is a remote sensing technique used to derive precise elevation measurements of the earth's surface (Ritchie 1995; Flood and Gutelius 1997; Wehr and Lohr 1999). It has been used in a limited number of geoscience applications, including the analysis of river networks (Kraus and Pfeifer 1998; Gomes Pereira and Wicherson 1999; Stock et al. 2005), the generation of river floodplain cross-sections (Charlton et al. 2003), the investigation of landslides (McKean and Roering 2004), and the mapping of tectonic fault scarps (Harding and Berghoff 2000; Haugerud et al. 2003), and bedrock contacts (Webster et al. 2006a). Webster et al. (2006a) used lidar data along with field observations to revise the bedrock geology and map three individual volcanic flow units within the North Mountain Basalt which were then used to categorize stream incision depths (Webster et al. 2006b).

In this study a high-resolution (ca. 4 m) laser altimetry (lidar) DEM was used to examine metrics of similar-size catchments that have been modified by glaciation. The Fundy Basin area was selected for this study because (i) the catchments are developed on three shallowly dipping volcanic flow units of the Jurassic North Mountain Basalt (NMB), each of which have uniform resistance to erosion (Figure 1), (ii) the area is tectonically inactive, (iii) the Bay of Fundy provides a uniform base level for all streams, (iv) there is a clear distinction in till cover thickness over the eastern and western portions of the study area, and (v) the age of deglaciation and subsequent fluvial erosion is well documented and uniform throughout the area. The local effects of the variable till cover on basin morphology and the interaction of surface and groundwater on net discharge and stream power were evaluated. This study benefited from previous work related to validating the accuracy of the lidar DEM (Webster 2005), and individual points (Webster and Dias 2006), mapping the basalt flow units (Webster et al. 2006a), and relating the stream incision depth to the basaltic flow units (Webster et al. 2006b). The objectives of this paper are to examine the morphology of several drainage basins derived from a high resolution lidar DEM to better understand landscape evolution of a section of North Mountain of the Bay of Fundy area in Nova Scotia. The effects of variable overburden thickness, rock type and drainage characteristics are evaluated with respect to landscape evolution. Drill core data of the NMB volcanic flow units were examined and fracture density measured to test the influence of bedrock fractures on erosion and drainage within each drainage basin. In addition, stream discharge and water chemistry were measured in two basins of similar size to determine the contribution of overburden to stream discharge.

PHYSIOGRAPHY AND AGE OF THE LANDSCAPE

The study area is situated along a 20-km section of North Mountain, mainland Nova Scotia, Canada, which comprises the eastern shore of the Bay of Fundy, known for the world's highest semi-diurnal tides. The Mesozoic Fundy Basin is predominantly underlain by Triassic sedimentary rocks (Blomidon and Wolfville Formations), conformably overlain by the Jurassic North Mountain Basalt (NMB) to the north and unconformably overlain by Paleozoic rocks of the Meguma Terrane to the south (Fig. 1). The NMB dips gently to the northwest, forms the

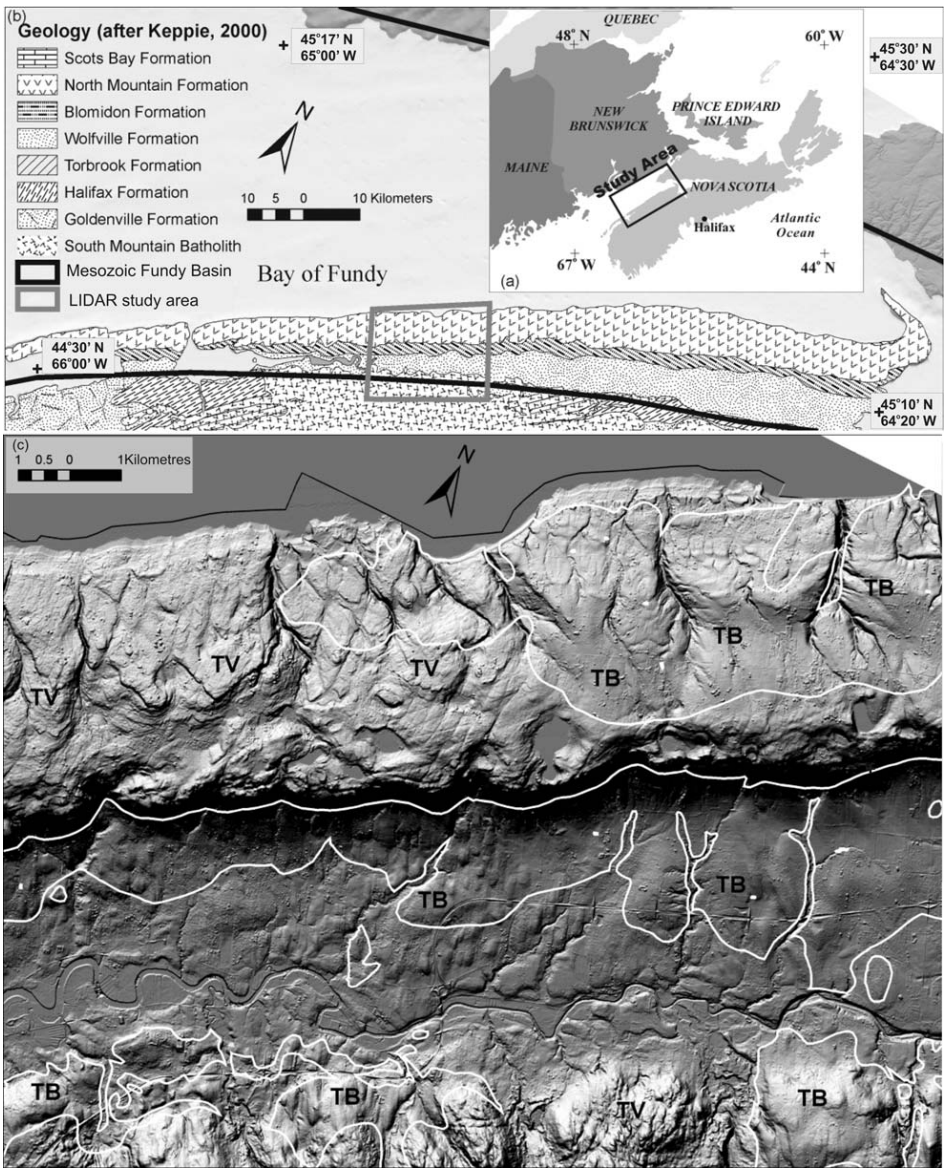

Figure 1. (a) Upper right study area location map (black rectangle). (b) Bedrock geology map (after Keppie 2000) of the Fundy Basin (heavy black rectangle) with lidar DEM location (heavy grey line). (c) Lidar DEM shaded relief model, azimuth angle 315, elevation angle 45; 5 times vertical exaggeration with the distribution of thick till blanket (TB) and thin till veneer (TV) (after Stea and Kennedy 1989).

southeast limb of a regional syncline (Withjack et al. 1995), and is crosscut by north to northeast-trending faults and fractures that exhibit dextral displacement (Olsen and Schlische 1990; Schlische and Ackermann 1995). The North Mountain Basalt consists of three distinct flow units (Kontak, 2002). The lower flow unit (LFU) consists of a thick (40–150 m) single, massive, coarse-grained flow. The middle unit (MFU) consists of multiple thin, fine- to coarse-grained, highly amygdaloidal flows (~3–15 m) with a cumulative thickness of 170–200 m. This is overlain conformably by a massive, coarse- grained upper flow unit (UFU) of variable, but poorly constrained, thickness (Kontak 2000; Pe-Piper 2000). The LFU is locally fractured and exhibits well- developed columnar jointing. A conjugate joint pattern is visible at the outcrop scale and on the shaded relief models of this flow (Fig. 1). The MFU is locally fractured and easily eroded when exposed at the surface, whereas the UFU has columnar joints that have been sealed with secondary minerals.

The maximum relief of the study area is 265 m (from sea level to the top of the North Mountain). The NMB dips approximately 6^{O} to the northwest (i.e., toward the Bay of Fundy) and on a regional scale, the land surface slopes at 3^{O} to 5^{O} in the same direction. The region has a modified continental climate strongly influenced by the adjacent Atlantic Ocean. Based on meteorological records from Environment Canada the annual mean precipitation is 1127 mm/yr, of which an average of 276 mm occurs as snow and 910 mm as rain. The wettest months are September and October when the average rainfall is 97 mm/month and the average daily temperature is 6.8^{O}C (Environment Canada 2005). The average daily temperature drops below zero in the month of December, reaches a minimum of -5.6^{O}C for the month of January, and rises above zero in the month of April. The land cover on the North Mountain is influenced by varying thicknesses of glacial till. Farmland (pastures and hayfields) and mixed forest dominate in the east where the till is thickest, whereas the land in the west is dominated by mixed forest cover. There are more roads and anthropogenic influences in the east compared to the west where only one paved road occurs along the coast. The topography of the coastline varies between gently sloping bedrock platforms and ca. 25 m cliffs that occur in embayments.

The region was affected by fluctuations in Late Wisconsinan ice dynamics until ca. 12 ka (^{14}C yr) (Stea and Mott 1998). The earliest ice flows were eastward and southeastward from an Appalachian or Laurentide ice source ca. 75-40 ka (Stea et al. 1998). The Hartlen Till was deposited as a result of the southeastward ice flow and typically consists of 40% gravel, 40% sand and 20% silt and clay (Lewis et al. 1998). The second major ice-flow was southward and southwestward from the Escuminac Ice Centre in the Prince Edward Island (PEI) region (Escuminac ice flow phase 2, ca. 22–18 ka; Stea et al. 1998). The resulting Lawrencetown Till (Stea et al. 1998) is a reddish muddy unit that has higher clay content than the underlying Hartlen Till due to the incorporation of Carboniferous red bed sediment

Table 1. North Mountain basin metrics derived from lidar DEM in Rivertools™. Catchment type: TV – till veneer; TR – transition zone; TB – till blanket. Drainage density* calculated from the stream network on the 1:10 000 scale topographic map.

Catchment Type	Area (km²)	Relief (km)	Stream Order	Drainage Density from DEM streams km/km²	Drainage Density* from mapped streams km/km²	Source Density from DEM streams streams/km²
Peck (TV)	4.52	0.067	9	293.71	1.65	20853.22
Phinneys (TV)	5.31	0.095	9	291.87	0.94	21906.91
Gaskill (TR)	7.81	0.085	9	292.30	1.38	19107.54
Hampton (TR)	2.03	0.049	8	295.86	2.9	21531.11
Chute (TR)	3.59	0.084	8	295.85	1.25	20472.35
Snow (TR)	4.11	0.095	9	294.91	1.12	19626.51
Poole (TR)	7.01	0.091	9	292.08	0.91	20016.68
Granville (TB)	4.23	0.053	9	293.01	1.39	22753.39
Sabeans (TB)	6.20	0.068	9	295.46	2.2	21405.68
Schoolhouse (TB)	3.63	0.056	9	291.89	1.42	23913.17
Starratt (TB)	7.66	0.077	9	293.07	1.34	20354.42

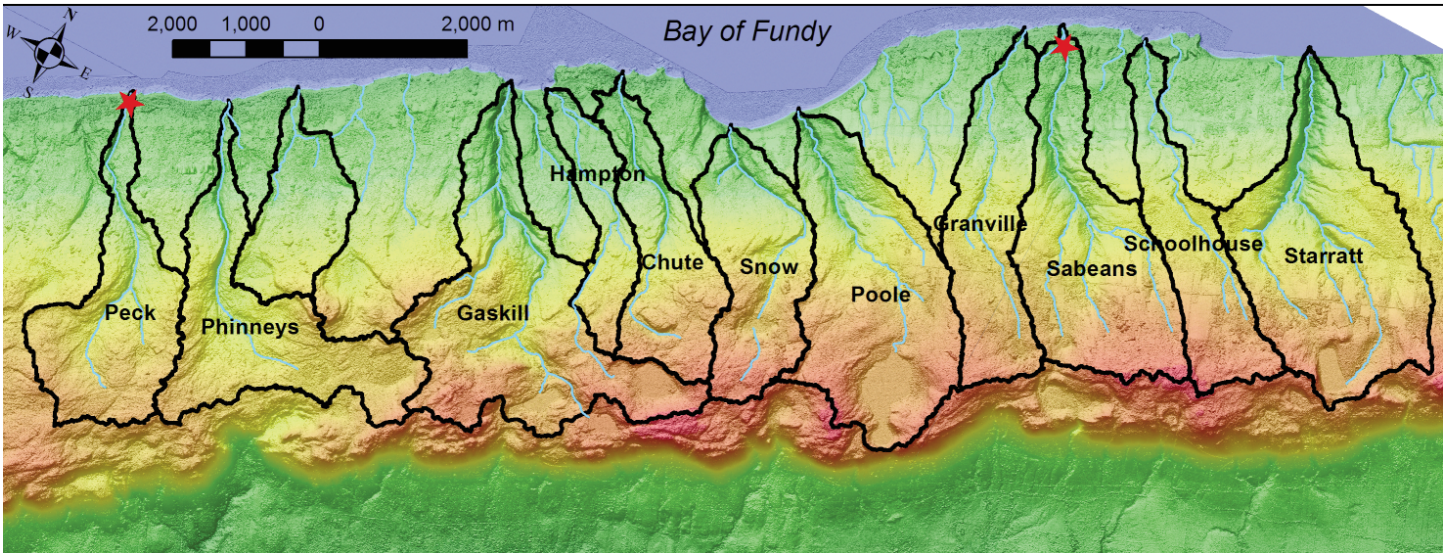

Figure 2. Labeled catchment basins (black lines) calculated from the lidar DEM for North Mountain. The blue lines denote the main truck streams within the basins. The two red stars denote the location of stream discharge and water chemistry sensors in Peck and Sabeans basins.

derived from Prince Edward Island, and typically consists of 20–30% gravel, 30–40% sand, and 30–50% silt and clay (Lewis et al. 1998). Ice then flowed northwestward and southward from the Scotian Ice divide across the axis of Nova Scotia at 18-15 ka (Stea et al. 1998). In a few localities, the Lawrencetown Till is overlain by a thin (1–4 m) hybrid till related to this event, known as the Beaver River Till, which generally consists of 50% gravel, 40% sand, and 10% silt and clay (Lewis et al. 1998). Locally ice flowed from the Scotian Divide northwestward over the NMB into the Bay of Fundy. With the late-glacial rise of relative sea level, ice flow into the Bay of Fundy increased to merge with southwestward ice streams from New Brunswick at ca. 13–12.5 ka (Stea et al. 1998). The study area was ice free by ca. 12 ka (Grant 1980).

The stratigraphy of the overburden in the study area is not well known. However, where overburden is present it is dominated by the Lawrencetown Till. In some areas thin post-glacial marine deposits mantle the till. Isolated kame and delta deposits also occur in the region. Soil development is poor with 'A horizon' thicknesses generally less than 30 cm. Stea and Kennedy (1998) describe the areas of thin < 1 m overburden as 'scoured bedrock' or a 'till veneer' (TV), which occur in the western catchments (Fig. 1), and the areas of thick > 1 m overburden as 'till blanket' (TB), which occur in the eastern catchments (Fig. 1). There is a transition zone between these two end-members, where catchments have a till veneer in their headwaters and a till blanket in their outlets.

The drainages on the Fundy side of NMB have evenly-spaced mainstems (1.5 km), similar catchment areas (ranging from 2 to 8 km²) and dendritic drainage patterns with stream densities ranging from 0.9 to 2.9 km/km² (Table 1; Fig. 2). The basins have streams which range in maximum stream order of 1 to 4 based on the method proposed by Strahler (1952). The basins with thicker till cover have higher order streams defined on the Nova Scotia Topographic Database

1:10 000-scale maps compared to the basins with thin till cover. The streambeds are typically 80% bedrock and 20% boulder-covered, and lack aggregation fluvial deposits. Till is present in the streambeds of some of the basins in the till blanket area, attesting to the youthfulness of these catchments and to the inheritance of some low relief, pre-glacial topography. The long profiles of the streambeds are ungraded and have several knick zones.

METHODS

Lidar and DEM Analysis

Details of the lidar data specifications and height validation results for this study are described in Webster (2005). Lidar data were acquired for the study area with an average ground point spacing of 2–3 m in open areas and 5–8 m in forested areas. Customized automated Arc/Info™ GIS routines for the validation of the lidar point data are available in Webster and Dias (2006). The height validation results indicate that the original lidar ground points and the derived DEM are, on average, typically within 15 cm of measured GPS heights and 95% of the data are within 30 cm for open hard surfaces (i.e. roads, parking lots). The lidar ground points were used to construct a 'bald earth' DEM at a 4 m resolution utilizing the ESRI suite of ArcGIS™ v. 8 and 9 software. A combination of Rivertools™ v. 3 and PCI Geomatica™ v. 9 software was used to extract the morphometric parameters from the drainage basins (Fig. 2).

Catchment basins were calculated for the main streams draining into the Bay of Fundy from the lidar DEM based on outlet locations identified on 1:10 000 scale topographic maps using Rivertools™. The resultant basin metrics are presented in Table 1. The standard D-8 algorithm (Jenson and Domingue 1988; Costa-Cabral and Burges 1994) was used to determine down stream flow direction and sinks (depressions within the DEM treated as errors by the algorithm) are filled in the DEM to allow continuous down stream flow. At most resolutions, care must be taken to consider that some landscape metrics are fractal, such as relief and slope (Anhert 1970; Van Der Beek and Braun 1998; Zhang et al. 1999). For this study the emphasis is on catchments with similar size so we have not chosen a fixed-scale averaging method—this allows us to examine the streams with maximum DEM resolution. However, when dealing with DEMS at high resolution, other considerations must be made regarding features such as sinks in the terrain model that are common in typical DEMs derived from photogrammetry. Inspection of the drainage basin boundaries and stream longitudinal profiles indicates that most catchments have sinks. Many of these sinks are adjacent to the raised elevations of a roadbed captured by the high resolution of the lidar DEM. As a culvert could not be represented on the DEM, a 'notch' was cut across the roadbed and assigned an elevation of the nearest downstream cell to improve the accuracy of the flow direction algorithm and to prevent excessive erroneous sink filling operations in deriving the catchment basins and stream profiles. This modification improved accuracy of the flow direction algorithm, prevented excessive erroneous sink-filling operations in deriving the catchment basins and stream profiles, and allowed the stream to 'pass through the roadbed.' The overall result is the generation of a more accurate flow accumulation grid and basin boundary.

Eleven catchment basins draining the NMB into the Bay of Fundy were extracted from the DEM using Rivertools™ (Fig. 2). Table 1 presents the morphometries of the extracted basins including drainage area, relief, maximum stream order from Rivertools™ drainage density from Rivertools™ and drainage density based on the streams mapped on the 1:10 000-scale Nova Scotia Topographic Database map series. The drainage density of the basins is similar, regardless of the stream order used in Rivertools™. Drainage densities calculated from the 1:10 000 topographic map stream networks showed more variability (denoted as Drainage Density * from mapped streams in Table 1).

Morphometric Analysis

Valley cross-sections, transverse to the overall basin slope and extending from the lateral drainage divides, were extracted for each of the basins in order to evaluate the incision depth using a method similar to that described in Montgomery (2002). Montgomery (2002) used the area of the cross-sections to calculate the incision depth and cross-section area between the drainage divides. Valley bottoms in the cross-sections were aligned midway upstream of each basin in order to facilitate a comparison in valley shape between the two basin end-members, the scoured bedrock and till blanket basins (Fig. 3). Integrated valley cross-sections were used to compute the volume of material removed from each basin as described in Mather et al. (2002). This approach assumes each cross-sectional area is representative of the erosion between cross-sections and is used to summarize the total volume of material eroded.

The elevations associated with the drainage divides were used to construct a paleosurface of the NMB following a similar method to that described by Brocklehurst and Whipple (2002) and Montgomery and López-Blanco (2003). The drainage divides that were calculated from the watershed extraction process were overlaid with the lidar DEM and elevations extracted. These elevations are assumed to represent regions of minimal erosion and were used to interpolate a surface that represents the paleo-terrain prior to erosion of the drainage basins. The lidar DEM was then subtracted from this paleo-terrain surface to form an erosion map in order to quantify the incision depth and volume of material removed by glacial-fluvial processes and the patterns of erosion for each basin. The area associated with each erosion depth range was calculated for each basin. The NMB flow units (Webster et al. 2006a, b) were used to calculate the percentage of each unit per basin and the associated erosion depth per flow unit per basin and are presented in Table 2.

Bedrock Resistance to Erosion

Sklar and Deitrich (2001) tested the strength of various rock types to erosion and related it to river incision into bedrock. In this study, the resistance of basaltic flow units to erosion by abrasion and plucking was tested. Litholog-

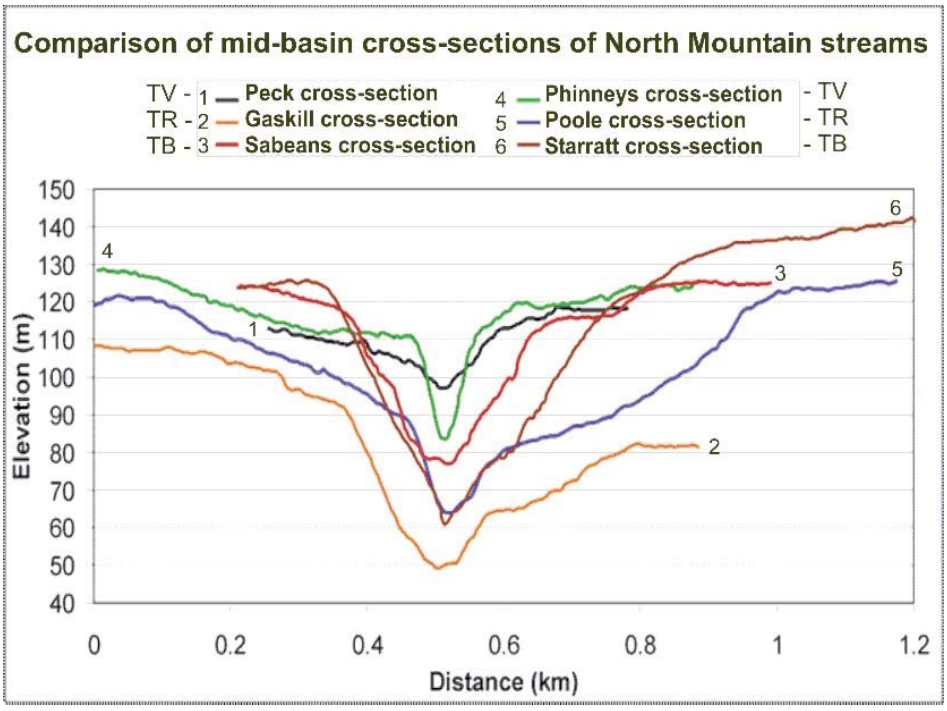

Figure 3. Mid-basin cross-sections of catchments from west to east on North Mountain with variable amounts of till cover. Cross-sections for the approximate midpoint of each basin are labeled: 1 – Peck, 2 – Gaskill, 3– Sabeans, 4 – Phinneys, 5 – Poole, and 6 – Starratt.

ical resistance to erosion by abrasion was tested in laboratory experiments on basalt flow unit samples using a shatterbox that consists of a cylindrical container that holds a central disk and an outer ring. Samples were crushed and sieved to between 2 and 5 mm in diameter and placed in the shatterbox which was agitated for times ranging from 2–15 minutes for samples from the MFU to 20 to 40 minutes for those from the UFU and LFU based on their resistance to abrasion. The samples were weighed prior to agitation in the shatterbox, then sieved and weighed after a set time of agitation to measure the change. The results of the shatterbox experiments are presented in Table 3.

Potential erosion by plucking was quantified by measuring the degree of fracturing in the basalt. Lineaments observed on the shaded relief lidar DEM maps (e.g. Fig. 1) and aerial photos are large-scale fractures that do not appear to control erosion in the streambed. Consequently drill cores of the MFU and LFU of the NMB were used to quantify the fracture density at a smaller scale and the distribution of vesicles and zeolite-bearing amygdules. Approximately 210 m of basalt were recovered from drill hole GAV-77-3 located 20 km east of the study area (Comeau 1978). The distinction between individual flows was based on the degree of oxidization of the flow and the amount of vesicles and amygdules of different sizes and characteristics (i.e., large or small, stratified or bubble pipes). Magnetic susceptibility and rock quality designation (RQD), an engineering property that computes the percentage of cumulative length of core segments longer than 10 cm over a 1 metre interval and the number of fractures were measured for every metre of core.

Surface and Groundwater Interaction

The effect of glacial till cover on surface water and groundwater interaction and stream discharge was evaluated by computing hydrographs and measuring water chemistry parameters in two of the catchments with contrasting thicknesses of till cover. These catchment basins, which were selected because they represent basin-type end-members, scoured bedrock till veneer (TV) and till blanket (TB), are of comparable size (Table 1). Thus, they can be used to test whether or not drainage area is an appropriate surrogate meas-

Table 2. Basalt flow unit percentage per catchment, average stream incision depths for each flow unit per catchment, overall average incision depth per catchment, and incision rate per catchment assuming a start time at 12 ka(thousands of years). TV – till veneer, TR transition between till veneer and till blanket, TB – till blanket. Incision rate km/Ma – km (kilometres) per Ma (millions of years).

Catchment	% Drainage area LFU	Incision depth (m) LFU	% Drainage area MFU	Incision depth (m) MFU	% Drainage area UFU	Incision depth (m) UFU	Average incision depth (m)	Maximum incision rate (km/Ma)
Peck (TV)	38.4	15.2	39.3	35.7	22.4	16.8	23.4	2.0
Phinney (TV)	62.5	35.4	17.4	38.8	20.1	11.3	28.5	2.4
Gaskill (TR)	54.0	35.2	27.4	54.2	18.6	31.8	42.3	3.5
Poole (TR)	68.4	27.1	30.5	52.2	1.2		44.6	3.7
Sabeans (TB)	45.5	25.8	21.1	43.5	33.1	16.6	32.4	2.7
Starratt (TB)	53.8	34.2	42.8	46.5	3.4		37.9	3.2
Average incision depth (m) per flow unit		28.8		45.2		19.1		

Table 3. Shatterbox experiment results for the North Mountain Basalt flow units. Upper flow unit (UFU), middle flow unit (MFU), lower flow unit (LFU), and weight percent (Wt %) of original sample for each sieve size in millimetres (mm). The time each sample was agitated in the shatterbox is reported in minutes (min).

Time (min)	>2 mm	>1mm	>0.5mm	>0.25mm	>0.125mm	>0.0623mm	<0.0623mm	Sample	Rock_type
5	58.06	12.10	5.78	4.49	4.80	6.40	8.37	PC48	UFU
10	66.87	8.65	5.17	4.39	4.32	4.43	6.17	AR5	UFU
20	0.00	0.00	0.00	8.58	25.32	30.30	35.80	AR5	UFU
2	63.65	10.20	5.50	4.90	4.84	4.87	6.04	BT17	MFU
5	53.60	14.45	6.68	5.43	5.34	5.74	8.76	BT17	MFU
10	53.20	14.91	6.58	5.22	7.63	3.76	8.70	BT17	MFU
15	0.00	0.00	0.00	9.43	62.68	6.67	21.22	BT17	MFU
2	31.80	21.25	10.76	7.77	7.39	7.08	13.95	PC49	MFU
3	6.56	6.62	9.90	14.35	14.91	17.29	30.38	PC49	MFU
5	54.69	14.67	6.59	4.90	4.60	4.83	9.71	PC52	LFU
10	3.55	6.17	10.44	15.35	12.95	23.07	28.47	PC52	LFU
15	73.19	7.75	4.24	3.61	4.44	2.86	3.92	AR3	LFU
25	71.57	8.57	4.44	3.84	3.68	3.74	4.15	AR3	LFU
40	55.42	12.24	7.43	6.48	6.28	6.71	5.44	AR3	LFU

ure for discharge in glaciated terrains. The thin TV cover is represented by the Peck Brook catchment and the thick TB cover is represented by the Sabeans Brook catchment (Fig. 2). The streams in each catchment were measured to record hourly stream discharge and water chemistry parameters from April to July 2004. Pressure transducers were placed in or near culverts to record stream stage near the outlets of Peck Brook and Sabeans Brook catchments (locations shown by red stars in Fig. 2). Manning's equation was used to calculate flow velocity and convert stream stage to discharge for the two channels (e.g. Rose 2004). Multimeters were also deployed near the outlet of these two basins to record water chemistry parameters, temperature, pH, specific conductance, dissolved oxygen, and turbidity. Meteorological stations were deployed throughout the Annapolis Valley and on North Mountain to measure meteorological events which were correlated with the stream data. The stream discharge, water chemistry and meteorological conditions were integrated and stream hydrographs were constructed for the two basins. The hydrographs were normalized by basin drainage area as reported in Tague and Grant (2004).

RESULTS

Lidar and DEM Analysis

The enhanced spatial resolution of lidar and the ability to penetrate the vegetation canopy allow subtle topographic features to be highlighted. The colour shaded relief (CSR) DEM was compared to the established surficial geology boundaries and glacial striation directions (see Stea and Kennedy 1998) (Fig. 4a). The contrast in terrain roughness from west to east on North Mountain is visible on the DEM (Figs.1, 4). The rough terrain in the western region of North Mountain correlates with glacially scoured bedrock, and the smoother terrain in the eastern region correlates well with surfaces covered by the Lawrencetown Till (Stea and Kennedy 1998) (Fig. 4a, b). Two previously unidentified glacial landforms are evident on the valley floor based on the CSR DEM (Fig. 4c). These landforms represent a set of oval shaped drumlins trending 155^{o} –355^{o} and a set of streamlined landforms trending 132^{o} –312^{o}. Based on field verification, the set of oval landforms in the western region, with a long axis trending ca. 335^{o} are composed of Lawrencetown Till draped by a thin layer of glacial marine lacustrine clay. The set of streamlined landforms in the eastern region, which has a long axis trend ca. 312^{o} is also visible on the DEM maps (Fig. 4) and are composed of Lawrencetown Till. Streams on the eastern flank of the North Mountain, where there is till cover, have flow directions of 312^{o}, parallel to the streamlined landforms in the valley (Fig. 4).

Morphometric Analysis

Representative cross-sections of the TV basins generally exhibit steep valley sides with flat bottom valley floors, whereas the till blanket (TB) basins commonly have lower valley slopes and wider valley bottoms (Fig. 3; see Table 1 for a complete list of basin names and amount of overburden). The TV basin valleys have broad gentle slopes in their headwaters and narrow steep valleys closer to their outlets where they are incised into the more resistant LFU. The TB basins have lower slopes and wider valley bottoms along their entire length (Fig. 3).

An erosion map highlights the differences in morphometry between the scoured bedrock and till blanket basins and the flow units of the NMB (Fig. 5). The TV basins have narrow incised valleys along their entire length and consist of only one main stream reach. The TB basins occur in broader valleys with larger tributaries. Table 1 shows the area and relief of each basin along with the drainage density calculated from the DEM and from the 1:10 000-scale mapped streams denoted with an * in the table. The drainage density calculated from the lidar DEM in Rivertools™ is similar for all basins (Table 1). However, the drainage density is lowest in the basins with thin till cover when the mapped streams are used (Drainage density *, Table 1). This is consistent with the higher maximum stream order of mapped streams (orders 3–4) of the basins which have

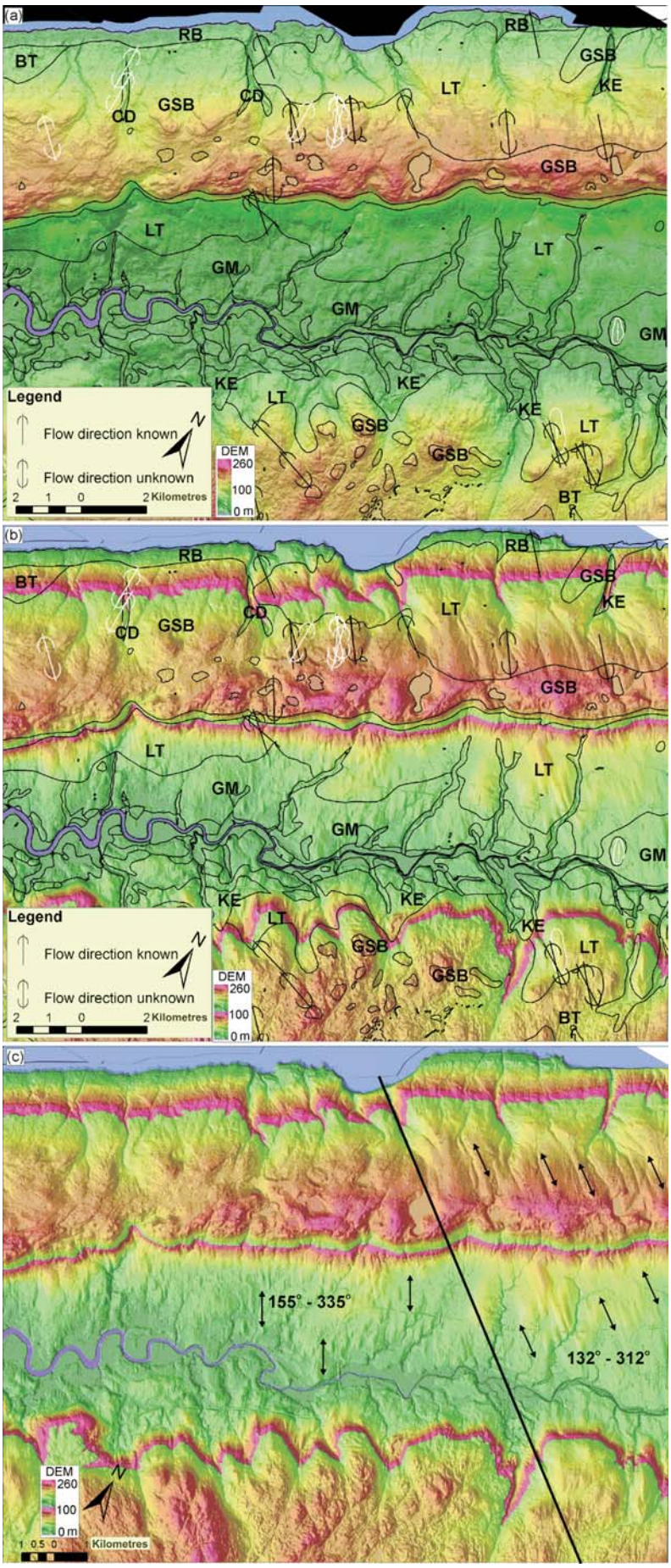

Figure 4. Colour shaded relief DEM maps (a and b) compared with surficial geologic boundaries and glacial striations (black symbols from Stea and Kennedy (1998) and white symbol striations from this study). (a) Standard chromostereoscopic colour coding of the DEM to enhance overall terrain features and relief, shading azimuth angle from 315° and zenith angle 45° with a five times vertical exaggeration. (b) Same colour ramp as above except it is scaled from 0–100 m, then repeated in order to enhance the subtle topographic features at lower elevations; shading azimuth angle changed to 225° to enhance northwest-trending glacial landforms. (c) Same image as (b) with the landform trends highlighted by double headed arrows. The field of oval-shaped landforms trend 155–335°, and the streamlined landforms in the east trend 130–310°. The terrain on both mountains east of the heavy line is smoother than the terrain to the west of the line. Surficial geology map labels: RB - raised beach deposits; GSB– glacially scoured bedrock; LT – Lawrencetown Till; GM – glaciomarine lacustrine deposits; BT – Beaver River Till; KE – kame fields and esker systems; CD – colluvial deposits.

thicker till cover compared to those of thin till (orders 1–2). The difference between the drainage density derived from the DEM and that from the mapped stream network is related to the fact that artificial and ephemeral streams are constructed from the DEM which are not represented on a topographic map as streams. Table 2 highlights the areal percentage of the basalt flow units for the three basin till cover groups (TV, TR, and TB) and complements the spatial patterns observed in Figure 5. The average incision depth for each basaltic flow unit within each basin is also presented along with the average incision depth for each basaltic flow unit based on all of the basins and for each entire basin (Table 2). The average incision depth is the least for the TV basins (Peck 23.4 m and Phinneys 28.5 m) in the west and increases eastward. The maximum

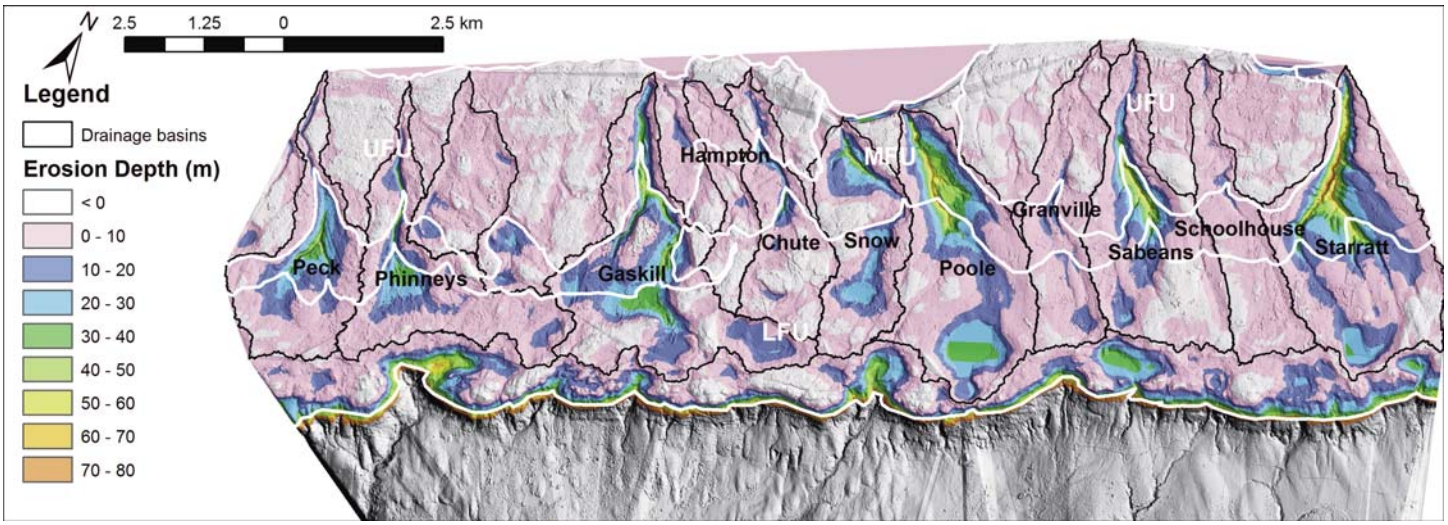

Figure 5. North Mountain drainage basin boundaries (black lines and labels) and erosion depth map with basalt flow unit boundaries (white lines and labels: Lower Flow Unit – LFU, Middle Flow Unit – MFU, Upper Flow Unit - UFU). The western basins have maximum incision depths of approximately 40 m and the central and eastern basins have maximum incision depths approaching 80 m.

average incision depths are associated with the basins within the transition zone of till thickness (TR) for Gaskill and Poole basins at 42.3 m and 44.6 m respectively. The average incision depths for the TB basins (Sabean 32.4 m and Starratt 37.9 m) falls between the incision depths of the till veneer and transition basins. The MFU lithology has the deepest incisions depths for all basins, regardless of till cover thickness, with an average of 45. 2 m. The LFU has an average incisions depth of 28.8 m for all of the basins and is more resistant than the MFU. The UFU does not occur in all the basins; however it shows the lowest average incision depth of 19.1 m. Maximum incision rates have been calculated for the catchments based on the following assumptions: (1) fluvial incision began after deglaciation, reported to be at 12 ka ± 220 yrs by Stea and Mott (1998), and (2) the till cover was originally flat. The rates are maxima because the tills probably had some relief and incision may have started prior to this time. The rates represent preferential erosion of till relative to bedrock. These rates can vary up to 12.4% based on the accuracy of the methods used to calculate incision depth and the date of deglaciation. The maximum incision rate is highest in the catchments within the transition zone at 3.7 and 3.5 km/Ma, followed by the catchments covered by the thick till blanket at 3.2 – 2.7 km/Ma and lowest for the catchments covered by a thin till veneer at 2.4 – 2 km/Ma (Table 2).

Statistics associated with the erosion depth map (Fig. 5) include the areal extent and the volume of material removed for each catchment (Fig. 6). The erosion depth map is the difference of the DEM with a paleo-surface constructed from the elevations of the drainage divides. The individual NMB flow units have been overlaid to indicate the differences in erosion related to the variable resistance to erosion of the flow units which is discussed in more detail in the next section (Fig. 5). The TV basin end-members (Peck and Phinneys Brook catchments) show the lowest area and volume of erosion with the TR and TB basins showing the highest area and volume of erosion (Fig. 6). The most sediment removed is from the Starratt Brook catchment, which is covered by a thick till blanket (Figs. 5, 6). The volume of sediment removed for the rest of the catchments follows a similar trend as the incision depths (Fig. 5), with the catchments within the transition zone having the most sediment removed and the least sediment removed in the thin till cover catchments (Fig. 6).

Bedrock Resistance to Erosion

The bedrock resistance to erosion influences the incision depth as can be seen in Fig. 5. The average incision depth is greatest for the Middle Flow Unit at 45.2 m, followed by the Lower Flow Unit at 28.8 m and the Upper Flow Unit at 19.1 m (Fig. 5; Table 2). There does not appear to be a pattern relating incision depth and the amount of overburden for the LFU (Table 2). However, the MFU has the greatest erosion depths in the basins with some glacial till cover. The maximum erosion depth in the MFU occurs in the transition catchments (TR) where till occurs in the upper parts of the watershed, followed by the catchments covered by a till blanket (TB) and are lowest in the thin till veneer (TV) catchments (Fig. 5; Table 2). A similar pattern is observed for the erosion of the UFU where erosion depth is greatest in the TR catchments, followed by the TB and lowest in the TV catchments. It appears that thick till cover in the upper section of the watershed is important to possibly provide tools for erosion downstream.

As indicated by experimental results (Table 3), the MFU is much more susceptible to erosion by abrasion than the UFU and LFU. For example, after 10 min. of abrasion, MFU sample BT17 had over 50% of the sample greater than 2 mm in diameter, whereas after 2 minutes of abrasion MFU sample PC49 only had 32% of the sample greater than 2 mm diameter after 2 min. (Table 3). The resistance of the MFU is variable

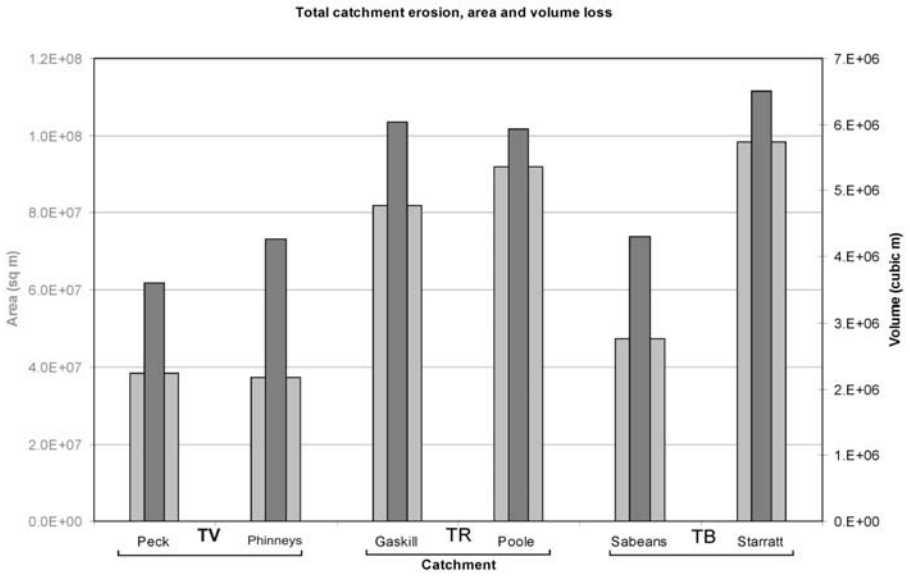

Figure 6. Graph of area and volume of erosion for each basin along the North Mountain Basalt. The basins have been grouped based on the degree of glacial till cover: TV – thin till veneer, TR – transition zone with till in the headwaters, and TB – thick till blanket. The thicker light grey bars represent total area (left axis) of material removed per basin and the thinner dark grey bars represent the total volume (right axis) of material removed per basin.

depending on the density of vesicles and amygdules. Drill core analysis shows that the highly vesicular and amygdaloidal MFU has a higher rock quality designation (RQD) than the LFU, indicating a higher percentage of rock segments longer than 10 cm (Fig. 7). The UFU and LFU broke down at similar rates and are significantly more resistant to abrasion than the MFU. The LFU has a greater number of fractures per metre than the MFU and a lower RQD indicating fewer segments greater than 10 cm in length per metre. The UFU does not occur in the drill core, however field observations indicate that secondary minerals have sealed fractures in this unit and that erosion by plucking is less prevalent in this unit than in the MFU or LFU. The results of the stream incision calculations for each basin are consistent with the shatterbox experiments which show the MFU is the least resistant to erosion followed by the ULF and LFU. The variation in stream incision depths appears to be related to several characteristics of the bedrock lithologies including the resistance to abrasion, the frequency and spacing of fractures, and the occurrence of bedding planes between flows (Fig. 7). Based on field observations of plucking in the streambed, the high fracture density of the LFU controls erosion for this unit (Fig. 7). Erosion of the MFU is controlled by fractures and bedding planes associated with thinner flows and its susceptibility to abrasion that correlates with the concentration of vesicles and zeolite-filled amydgules as observed in the drill core (Fig. 7).

Surface and Groundwater Interaction

The normalized hydrographs of Peck Brook (TV) and Sabeans Brook (TB) catchments indicate that discharge after a rainfall event is much higher in the Sabeans Brook catchment (e.g. 0.75 m^3/km^2 sec on 4/23/2004) than in the Peck Brook catchment (e.g. 0.05 m^3/km^2 sec on 4/23/2004) (Fig. 8a). The response time of the hydrographs between the two catchments is similar. However, the normalized discharge of Sabeans Brook is greater than Peck Brook and may be attributed to different rates of evapotranspiration between the catchments, because the Peck Brook catchment has more forest cover and less cleared agricultural land than the Sabeans Brook catchment. The water in Sabeans Brook is generally more turbid after a rain than in Peck Brook. However, after a significant rain event the specific conductance in Sabeans Brook decreases, whereas it increases in Peck Brook (Fig. 8b). Based on the hydrographs, Sabeans Brook receives more overland flow than Peck Brook after a rain. The dominant hydrologic process of overland flow for Sabeans Brook catchment and infiltration for Peck Brook catchment is consistent with the water chemistry data (Fig. 8b). The higher turbidity in Sabeans Brook compared to Peck Brook is likely the result of till material washing into the stream. The decrease in specific conductance of the water in Sabeans Brook after a rain event is considered to represent dilution, and the increase in Peck Brook is representative of increased base flow of water that has had a longer residence time in contact with the bedrock (Hem 1985; Winter et al. 1998). The dominant process of overland flow in the Sabeans Brook catchment compared to infiltration in the Peck Brook catchment is attributed to the lower permeability of the Lawrencetown Till that covers the Sabeans Brook catchment area.

DISCUSSION

The streamlined landforms in the valley floor and the alignment of the upper reaches of streams in the till blanket (TB) catchments are likely to be a result of the Scotian ice phase, which appears to have been the last ice advance to affect this area (Stea and Mott 1998). The streamlined landforms and distribution of till suggests that an ice stream may have flowed from South Mountain across the valley into the Bay of Fundy (e.g. Stokes and Clarke 2001). The larger catchments are associated with thicker till cover (Fig. 2; Table 1). The variation in sediment volume removed in these catchments (Fig. 7) is consistent with the variation in morphometric measurements (Figs. 3, 5). The maximum mapped stream order is lowest in the basins with thin till and highest in the transition zone and basins with thicker till. This may be a combination of the till being easier to erode and the influence of the ice stream to form topographic depressions that have been used as preferential pathways for the streams.

Others (Kirkbride and

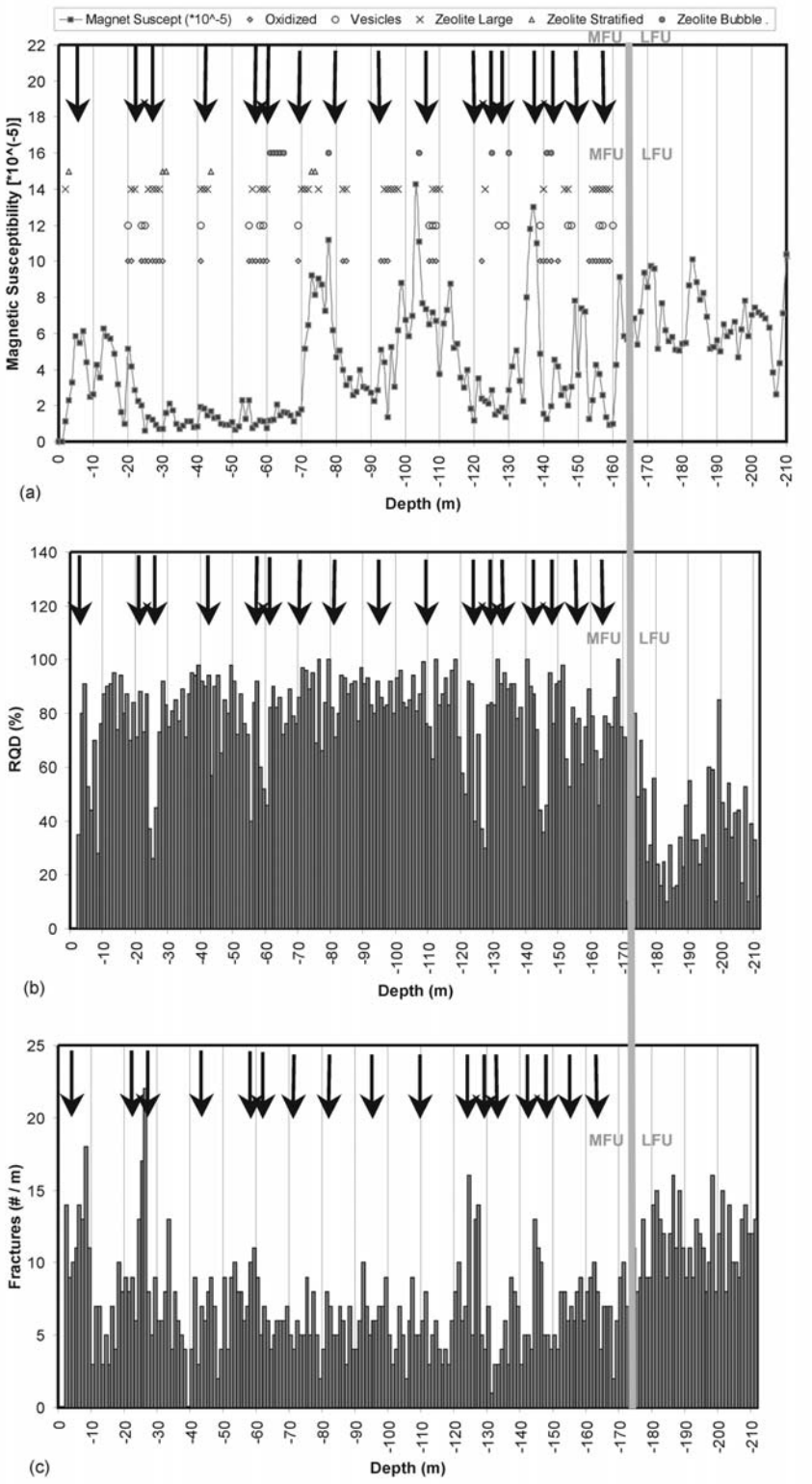

Figure 7. Plots of drill core logs of drill hole GAV77–3 for the North Mountain Basalt. The heavy grey vertical line marks the contact between the Middle Flow Unit (MFU) and Lower Flow Unit (LFU). (a) Magnetic susceptibility and the distribution of oxidized basalt, vesicles and amygdules interpreted to represent flow tops. The arrows denote individual flows within the MFU. The boundary between the MFU and LFU occurs at depth 162 m. (b) Rock Quality Designator (RQD) %, which is the cumulative percentage of the number of pieces of core that are larger than 10 cm over a distance of 1 m. (c) Number of fractures per metre length of core.

Matthews 1997; Li et al. 2001) have examined valley cross-sections to show differences in shape between glaciated and non-glaciated valleys. In this study, the glacial processes appear to have over-deepened and widened the catchments in the eastern region of the study area where the till blanket is thickest (Figs. 3, 5; Hallet et al. 1996). Differences in basin morphology appear to be in part related to the variable till thickness and its influence on surface and groundwater interaction, which in turn has a strong effect on stream power. The erosion depth map shows the combined effect of variable bedrock lithology on stream incision and the effect of glacial till cover on basin morphology (Fig. 5). This indicates that the basins in the transition zone and those with thick till cover are more deeply incised than the scoured bedrock catchments and the till blanket catchments have the best developed drainage systems (Figs. 5, 6). The till blanket catchments have more tributaries contributing to the main trunk stream than the till veneer catchments (Fig. 5; Table 1). These tributaries likely form because overland flow is accentuated in the thick till blanket catchments due to high clay contents and associated low effective permeability of the sediment. This is consistent with the observed stream discharge and water chemistry (Fig. 8). The variable resistance to erosion of the basaltic flows results in the MFU unit having the greatest incision depths (Table 2). This is attributed to the highly fractured and amygdaloidal character of this basaltic flow as demonstrated in the abrasion tests and analysis of the fractures in the drill core (Table 3; Fig. 7). Several boulders of resistant LFU basalt occur in the stream beds of all basins. We believe these boulders act as tools in the abrasion of the stream bed basalts. The occurrence of these tools in the transition basins where till occurs in the upper watershed and the glacial till blanket basins promote erosion and the MFU has the greatest erosion depths for these catchments. The MFU also has a density of fractures which promotes erosion by plucking and contributes to the deeper incision depths for this unit. As a result, the MFU has undergone the deepest incision which is attributed to the high susceptibility

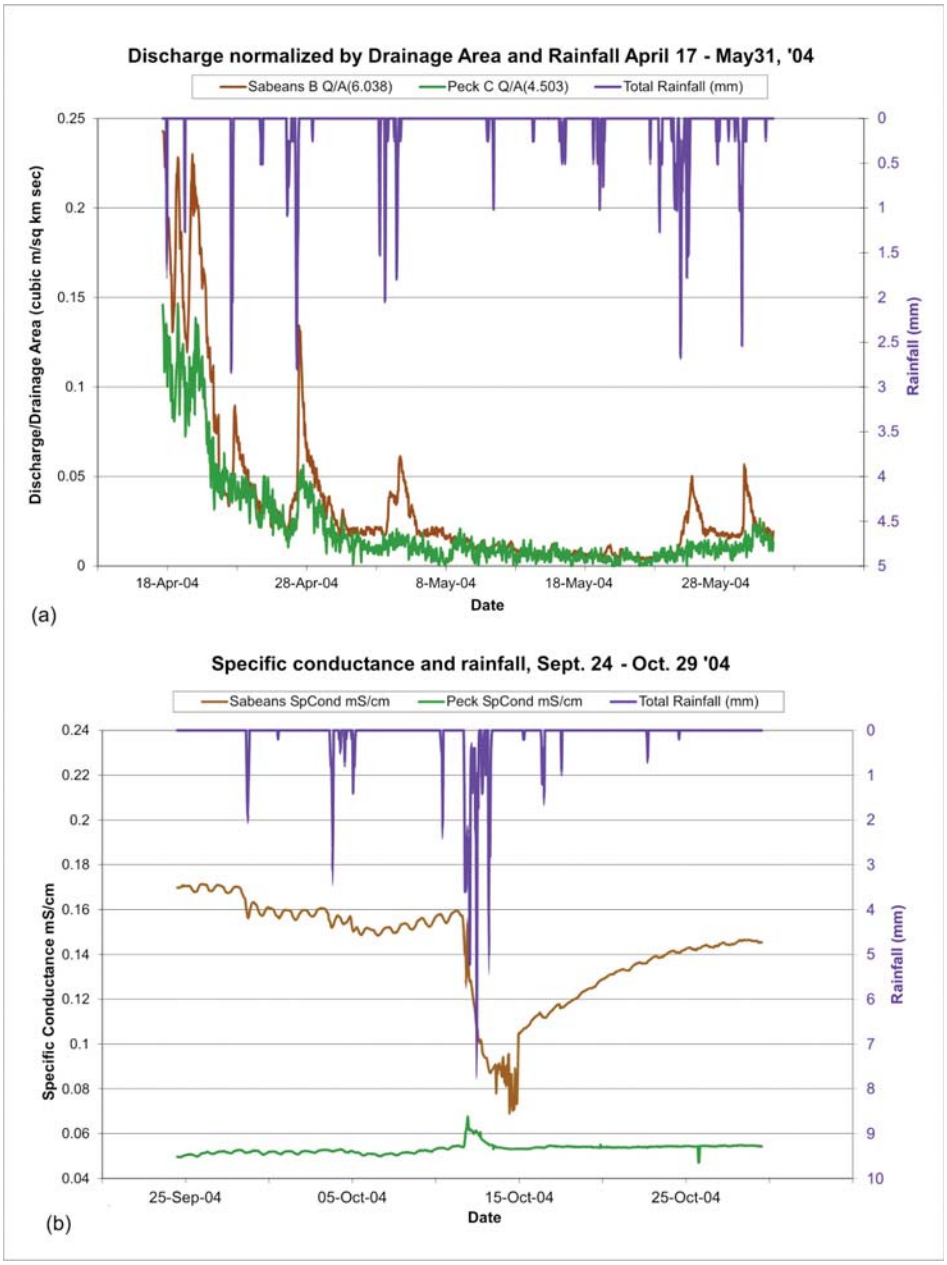

Figure 8. Hydrographs and water chemistry plots of representative basins from the till blanket (TB) area (Sabeans Brook catchment dark grey) and the scoured bedrock till veneer (TV) area (Peck Brook catchment light grey). (a) Hydrographs of Sabeans Brook and Peck Brook basins, discharge m^3/s normalized by basin drainage area (km^2) for the period of April 17 to May 31, 2004. Rainfall (mm) is plotted in reverse order on the right y-axis. (b) Specific conductance (microseimens per centimetre) and rainfall for Sabeans Brook and Peck Brook for the period of September 24 to October 28, 2004.

of this unit to break down through abrasion and plucking.

Pazzaglia et al. (1998) noted that stream power can control the shape of the stream longitudinal profile and that discharge is influenced by the drainage area and infiltration characteristics of the basin. Many studies have used drainage area as a surrogate measure of stream discharge (Sklar and Dietrich 1998; Snyder et al. 2000; Kirby and Whipple 2001; Whipple and Tucker 2002; Mather et al. 2002; Finlayson and Montgomery 2003; Stock et al. 2005) in estimating stream power (Equation 1). Montgomery (2002) used drainage area as a normalizing parameter to compare metrics of valleys affected by variable degrees of glaciation. Where basins are being compared, the use of drainage area to estimate discharge assumes that hydrologic processes affecting discharge in those basins are similar. Although this assumption may be true at a regional scale (1000 km^2 and larger), the results of this study indicate that there can be significant variations in hydrologic processes between basins within a region (< 100 km^2) and that drainage area may not accurately correlate to discharge and consequently to stream incision. Monitoring the hydrographs and water chemistry of catchments from two basins with contrasting amounts of glacial till and land cover demonstrate the strong influence that till thickness and sedimentology has on runoff and stream discharge. The differences in the hydrographs are a result of the amount and rate of delivery of surface runoff for each catchment to the stream. The till blanket catchments promote surface runoff (overland flow) because of the low permeability of the till, whereas the scoured bedrock promotes infiltration and delivers water more gradually to the stream through base flow. This is consistent with the findings of Tague and Grant (2004) who observed that hydrographs from basins in older weathered volcanic rocks exhibiting low intrinsic permeability were much 'flashier' than those with younger, more permeable volcanic rocks in the Cascades of Oregon.

The Lawrencetown Till has a high silt and clay content (30-50%) and low permeability (< 10^{-6} cm/sec) making it suitable for liners in landfill sites and other structures that require low permeable material (Lewis et al. 1998). Although there are no direct permeability measurements for the basalt flow units that we are aware of, the MFU and LFU are highly fractured which would result in higher intrinsic permeability's (Fig. 7). Haan et al. (1994) reported a range of hydraulic conductivities for fractured basalt to be between 10^{-6} and 10^{1} (m/day) and glacial till to be between 10^{-7} and 10^{0} (m/day) and clay between 10^{-7} and 10^{-3} (m/day). Rose (2004) reported hydraulic conductivities for fractured bedrock to be between 10^{-8} and 10^{-4} (m/sec) and clay to be between 10^{-10}

and 10^{-8} (m/sec).

Pump tests from water wells within the basalt aquifer yield an average of 14.4 imperial gallons per minute (10 wells) and are prone to surface contamination where the till cover is thin (D. Fanning, pers. comm. 2004). These data further support our interpretation that the low permeable till blanket promotes surface runoff and the scoured fractured bedrock permits infiltration of precipitation. With increased overland flow, more water enters the stream more quickly after a rain and increases the overall discharge and stream power, thus enhancing the stream's ability to erode. This study demonstrates that in glaciated terrains, factors such as a till thickness and sedimentology can affect the hydrologic properties of a catchment and consequently the morphology of the drainage basin. The high degree of variability in surface and groundwater interaction that can occur within a relatively small area can strongly influence the nature of stream discharge. This has important implications for water quality and quantity in glaciated terrains.

SUMMARY

Landscapes within the study area are typical of those found in northeastern North America that have been significantly eroded. The terrain is also representative of many areas in the world that have been eroded by fluvial process for millennia and during the Quaternary by glacial processes. This area is an ideal site to examine factors controlling landscape evolution. The catchments are all generally the same size, are underlain by similar lithologies with relatively simple structures, and have experienced the same changes in base level. This facilitates an examination of the effects of glacial till within a region on moderate-scale catchments. Studying the morphology of catchments at this scale allows examination of factors affecting hydrologic and geomorphic processes that can be used to scale up to larger basins.

Airborne terrestrial lidar has been a valuable tool in the analysis of these moderate-scale catchments and stream morphology within a forested region. In addition to basin morphology, the ability of the laser system to generate high-resolution precise terrain heights in heavily vegetated terrains has facilitated the identification of geologic contacts within the basalt units and the identification of new landforms interpreted to be related to late-stage ice dynamics and fluctuations in sea-level. The catchments with the thickest till cover have had the most sediment eroded from them and differ in their morphology compared to the scoured bedrock catchments. In addition, the catchments in the till blanket area have higher drainage densities and deeper fluvial incision depths. We attribute these differences in catchment morphologies to reflect the influence of glacial till on hydrologic and fluvial process and the possible addition of more tools in the streambed to promote erosion by abrasion. The till has a significant effect on the surface and groundwater interaction by promoting overland flow and retarding infiltration. The process of infiltration dominates the scoured bedrock catchments during precipitation where water is filtered through fractures into the groundwater table and released as base flow into the stream as is evident from the hydrographs and water chemistry. The MFU and LFU are both highly fractured with an average of 7 and 10 fractures per metre, respectively, allowing infiltration in the thin till catchments. In the catchments with thick till cover, the increased overland flow results in higher discharge and stream power per unit area compared to the thin till covered catchments. This has important implications in glaciated terrains if the drainage area is used as an approximate measure of discharge as is commonly the practice.

The results of this study are widely applicable to other glaciated terrains where vegetation cover obscures the topography. The ability of lidar to penetrate the vegetation canopy makes it an ideal tool for determining catchment morphologies in such areas.

ACKNOWLEDGEMENTS

We thank Ralph Stea and Dan Kontak of the Nova Scotia Department of Natural Resources for field visits and discussions. We also thank Alex Mosher, Adam Csank, and Daniel Roberts for assistance with the field work. Thomas Duffet of Dalhousie University kindly provided instructions on the use of the shatterbox, and Cliff Stanley of Acadia University made available the drill core GAV-77. The lidar data were supplied by the Applied Geomatics Research Group (AGRG) of the Nova Scotia Community College (NSCC) and was funded by a Canada Foundation for Innovation research grant from Industry Canada. TW also thanks Bob Maher for his flexibility allowing him time to work on this research. Financial assistance was provided by the National Sciences and Engineering Research Council (via JBM) and the NSCC to assist TW's PhD study. JCG acknowledges support from the Atlantic Canada Opportunities Agency – Atlantic Innovation Fund grant 1005052. We thank the two reviewers of this manuscript who provided important comments which have improved the manuscript.

REFERENCES

Anhert, F., 1970, Functional relationships between denudation, relief, and uplift in large, mid-latitude drainage basins: American Journal of Science, v. 268, p. 243–263, http://dx.doi.org/10.2475/ajs.268.3.243.

Brocklehurst, S.H., and Whipple, K.X., 2002, Glacial erosion and relief production in the Eastern Sierra Nevada, California: Geomorphology, v. 42, p. 1–24, http://dx.doi.org/10.1016/S0169-555X(01)00069-1.

Brocklehurst, S.H., and Whipple, K.X., 2004, Hypsometry of glaciated landscapes: Earth Surface Processes and Landforms, v. 29, p. 907–926, http://dx.doi.org/10.1002/esp.1083.

Charlton, M.E., Large, A.R.G., and Fuller, I.C., 2003, Application of airborne LIDAR in river environments: The River Coquet, Northumberland, UK: Earth Surface Processes and Landforms, v. 28, p. 299–306, http://dx.doi.org/10.1002/esp.482.

Comeau, R.L., 1978, Uranium, North Kingston, Kings County, Nova Scotia, Getty Mineral Company, Limited: Nova Scotia Department of Natural Resources Assessment Report 21H/02B 54-K20(1).

Costa-Cabral, M.C., and Burges, S.J., 1994, Digital Elevation Model Networks (DEMON): A model of flow over hillslopes for computation of contributing and dispersal areas: Water Resource Research, v. 30, p. 1681–1692, http://dx.doi.org/10.1029/93WR03512.

Dietrich, W.E., Bellugi, D.G., Sklar, L.S., Stock, J.D., Heimsath, A.M., and Roering, J.J., 2003, Geomorphic transport laws for predicting landscape form and dynamics, *in* Wilcock, P.R., and Iverson, R.M., *eds.*, Prediction in Geomorphology: Geophysical Monograph Series, AGU, v. 135, p. 103–132, http://dx.doi.org/10.1029/135GM09.

Environment Canada, 2005, Canadian Climate Normals: Government of Canada, Accessed May 10, 2005. http://climate.weather.gc.ca/climate_normals/.

Finlayson, D.P., and Montgomery, D.R., 2003, Modeling large-scale fluvial erosion in geographic information systems: Geomorphology, v. 53, p. 147–164, http://dx.doi.org/10.1016/S0169-555X(02)00351-3.

Flood, M., and Gutelius, B., 1997, Commercial implications of topographic terrain mapping using scanning airborne laser radar: Photogrammetric Engineering and Remote Sensing, (April 1997), p. 327–366.

Gao, J., 1997, Resolution and accuracy of terrain representation by grid DEMs at micro-scale: International Journal of Geographical Information Science, v. 11, p. 199–212, http://dx.doi.org/10.1080/136588197242464.

Gíslason, S.R., Arnórsson, S., and Ármannsson, H., 1996, Chemical weathering of basalt in southwest Iceland: Effects of runoff, age of rocks and vegetative/glacial cover: American Journal of Science, v. 296, p. 837–907, http://dx.doi.org/10.2475/ajs.296.8.837.

Gomes Pereira, L.M., and Wicherson, R.J., 1999, Suitability of laser data for deriving geographic information: A case study in the context of management of fluvial zones: ISPRS Journal of Photogrammetry and Remote Sensing, v. 54, p. 105–114, http://dx.doi.org/10.1016/S0924-2716(99)00007-6.

Grant, D.R., 1980, Quaternary sea-level change in Atlantic Canada as an indication of crustal deleveling, *in* Mörner, N-A., *ed.,* Earth rheology, isostasy, and eustacy: John Wiley and Sons, New York, p. 201–214.

Haan, C.T., Barfield, B.J., and Hayes, J.C., 1994, Design hydrology and sedimentology for small catchments: Academic Press, 588 p.

Hallet, B., Hunter, L., and Bogen, J., 1996, Rates of erosion and sediment evacuation by glaciers: A review of field data and their implications: Global and Planetary Change, v. 12, p. 213–235, http://dx.doi.org/10.1016/0921-8181(95)00021-6.

Harding, D.L., and Berghoff, G.S., 2000, Fault scarp detection beneath dense vegetation cover: Airborne lidar mapping of the Seattle fault zone, Bainbridge Island, Washington State (abstract): Proceedings of the American Society of Photogrammetry and Remote Sensing Annual Conference, Washington, D.C., p. 9.

Haugerud, R., Harding, D.J., Johnson, S.Y., Harless, J.L., Weaver, C.S., and Sherrod, B.L., 2003, High-resolution LiDAR topography of the Puget Lowland, Washington —A bonanza for earth science: GSA Today, v. 13, no. 6, p. 4–10.

Hem, J., 1985, Study and interpretation of the chemical characteristics of natural water: United States Geological Survey, Water-Supply Paper 2254, 225 p.

Jenson, S.K., and Domingue, J.O., 1988, Extracting topographic structure from digital elevation data for geographic information system analysis: Photogrammetric Engineering and Remote Sensing, v. 54, no. 11, p. 1593–1600.

Keppie, J.D., compiler, 2000, Geological Map of the Province of Nova Scotia: Nova Scotia Department of Natural Resources Minerals and Energy Branch, Map ME 2000-1, scale: 1:500 000.

Kirby, E., and Whipple, K., 2001, Quantifying differential rock–uplift rates via stream profile analysis: Geology, v. 29, p. 415–418, http://dx.doi.org/10.1130/0091-7613(2001)029<0415:QDRURV>2.0.CO;2.

Kirkbride, M., and Matthews, D., 1997, The role of fluvial and glacial erosion in landscape evolution: The Ben Ohau Range, New Zealand: Earth Surface Processes and Landforms, v. 22, p. 317–327, http://dx.doi.org/10.1002/(SICI)1096-9837(199703)22:3<317::AID-ESP760>3.0.CO;2-I.

Kontak, D.J., 2000, Nature of zeolite distribution in the North Mountain Basalt, southern Nova Scotia: field and geochemical studies, *in* MacDonald, D.R., and Mills, K.A., *eds.*, Minerals and Energy Branch Report of Activities 1999: Nova Scotia Department of Nature Resources, Report ME 2000-1, p. 105–124.

Kontak, D.J., 2002, Internal stratigraphy of the Jurassic North Mountain Basalt, Southern Nova Scotia: *in* MacDonald, D.R., *ed.*, Minerals and Energy Branch Report of Activities 2001: Nova Scotia Department of Nature Resources, Report ME 2002-1, p. 69–79.

Kooi, H., and Beaumont, C., 1996, Large-scale geomorphology: Classical concepts reconciled and integrated with contemporary ideas via a surface processes model: Journal of Geophysical Research, v. 101, p. 3361–3386, HTTP://DX.DOI.ORG/10.1029/95JB01861.

Kraus, K., and Pfeifer, N., 1998, Determination of terrain models in wooded areas with airborne laser scanner data: ISPRS Journal of Photogrammetry and Remote Sensing, v. 53, p. 193–203, http://dx.doi.org/10.1016/S0924-2716(98)00009-4.

Lewis, C.F.M., Taylor, B.B., Stea, R.R., Fader, G.B.J., Horne, R.J., MacNeill, S.G., and Moore, J.G., 1998, Earth science and engineering: Urban development in the Metropolitan Halifax Region, *in* Karrow, P.F., and White, O.L., *eds.,* Urban Geology of Canadian Cities: Geological Association of Canada Special Paper 42, p. 411–446.

Li, Yingkui, Liu, Gengnian, and Cui, Zhijiu, 2001, Glacial valley cross–profile morphology, Tian Shan Mountains, China: Geomorphology, v. 38, p. 153–166, http://dx.doi.org/10.1016/S0169-555X(00)00078-7.

Mather, A.E., Stokes, M., and Griffiths, J.S., 2002, Quaternary landscape evolution: a framework for understanding contemporary erosion, southeast Spain: Land Degradation and Development, v. 13, p. 89–109, http://dx.doi.org/10.1002/ldr.484.

McKean, J. and Roering, J., 2004, Objective landslide detection and surface morphology mapping using high-resolution airborne laser altimetry: Geomorphology, v. 57, p. 331–351, HTTP://DX.DOI.ORG/10.1016/S0169-555X(03)00164-8.

Montgomery, D.R., 2002, Valley formation by fluvial and glacial erosion: Geology, v. 30, p. 10471050, http://dx.doi.org/10.1130/0091-7613(2002)030<1047:VFBFAG>2.0.CO;2.

Montgomery, D.R., and López-Blanco, J., 2003, Post–Oligocene river incision, southern Sierra Madre Occidental, Mexico: Geomorphology, v. 55, p. 235–247, http://dx.doi.org/10.1016/S0169-555X(03)00142-9.

Olsen, P.E., and Schlische, R.W., 1990. Transtensional arm of the early Mesozoic Fundy rift basin: Penecontemporaneous faulting and sedimentation: Geology, v. 18, p. 695–698, http://dx.doi.org/10.1130/0091-7613(1990)018<0695:TAOTEM>2.3.CO;2.

Pazzaglia, F.J., 1993, Stratigraphy, petrography, and correlation of late Cenozoic middle Atlantic Coastal Plain deposits.

Implications for late-stage passive-margin geological evolution: Geological Society of America Bulletin, v. 105, p. 1617–1634, http://dx.doi.org/10.1130/0016-7606(1993)105<1617:SPACOL>2.3.CO;2.

Pazzaglia, F.J., 2003, Landscape evolution models: Developments in Quaternary Science, v. 1, p. 247–274, http://dx.doi.org/10.1016/S1571-0866(03)01012-1.

Pazzaglia, F.J., Gardner, T.W., and Merritts, D.J., 1998, Bedrock fluvial incision and longitudinal profile development over geological time scales determined by fluvial terraces, *in* Tinkler, K.J., and Wohl, E.E., *eds.*, Rivers Over Rock: Fluvial Processes in Bedrock Channels: Geophysical Monograph Series, v. 107, p. 207–235, http://dx.doi.org/10.1029/GM107p0207.

Pe-Piper, G., 2000, Mode of occurrence, chemical variation and genesis of mordenite and associated zeolites from the Morden area, Nova Scotia, Canada: The Canadian Mineralogist, v. 38, p. 1215–1232, http://dx.doi.org/10.2113/gscanmin.38.5.1215.

Ritchie, J.C., 1995, Airborne laser altimeter measurements of landscape topography: Remote Sensing of the Environment, v. 53, p. 91–96, http://dx.doi.org/10.1016/0034-4257(95)00043-Z.

Rose, C.W., 2004, An Introduction to the Environmental Physics of Soil, Water and Watersheds: Cambridge University Press, p. 226–258, http://dx.doi.org/10.1017/CBO9780511801426.008.

Schlische, R.W., and Ackermann, R.V., 1995, Kinematic significance of sediment-filled fissures in the North Mountain Basalt, Fundy rift basin, Nova Scotia, Canada: Journal of Structural Geology, v. 17, p. 987–996, http://dx.doi.org/10.1016/0191-8141(94)00114-F.

Seidl, M.A., Dietrich, W.E., and Kirchner, J.W., 1994, Longitudinal profile development into bedrock: An analysis of Hawaiian channels: The Journal of Geology, v. 102, p. 457–474, http://dx.doi.org/10.1086/629686.

Sklar, L., and Dietrich, W.E., 1998, River longitudinal profiles and bedrock incision models: Stream power and the influence of sediment supply, *in* Tinkler, K.J., and Wohl, E.E., *eds.*, Rivers Over Rock: Fluvial Processes in Bedrock Channels: Geophysical Monograph Series, v. 107, p. 237–260, http://dx.doi.org/10.1029/GM107p0237.

Sklar, L.S., and Dietrich, W.E., 2001, Sediment and rock strength controls on river incision into bedrock: Geology, v. 29, p. 1087–1090, http://dx.doi.org/10.1130/0091-7613(2001)029<1087:SARSCO>2.0.CO;2.

Snyder, N.P., Whipple, K.X., Tucker, G.E., and Merritts, D.J., 2000, Landscape response to tectonic forcing: Digital elevation model analysis of stream profiles in the Mendocino triple junction region, northern California: Geological Society of America Bulletin, v. 112, p. 1250–1263, http://dx.doi.org/10.1130/0016-7606(2000)112<1250:LRTTFD>2.0.CO;2.

Stea, R.R., and Kennedy, C.M., 1998, Surficial Geology of the Bridgetown area (NTS sheet 21A/14), Annapolis County, Nova Scotia: Nova Scotia Department of Natural Resources Minerals and Energy Branch, OFM ME 1998-2, scale 1:50 000.

Stea, R.R., and Mott, R.J., 1998, Deglaciation of Nova Scotia: Stratigraphy and chronology of lake sediment cores and buried organic sections: Géographie physique et Quaternaire, v. 52, p. 1–19.

Stea, R.R., Piper, D.J.W, Fader, G.B.J., and Boyd, R., 1998, Wisconsinan glacial and sea–level history of Maritime Canada and the adjacent continental shelf: A correlation of land and sea events: Geological Society of America Bulletin, v. 110, p. 821–845, http://dx.doi.org/10.1130/0016-7606(1998)110<0821:WGASLH>2.3.CO;2.

Stock, J.D., and Montgomery, D.R., 1999, Geologic constraints on bedrock river incision using the stream power law: Journal of Geophysical Research, v. 104, p. 4983–4993, http://dx.doi.org/10.1029/98JB02139.

Stock, J.D., Montgomery, D. R, Collins, B.D., Dietrich, W.E., and Sklar, L., 2005, Field measurements of incision rates following bedrock exposure: Implications for process controls on the long profiles of valleys cut by rivers and debris flows: Geological Society of America Bulletin, v. 117, p. 174–194, http://dx.doi.org/10.1130/B25560.1.

Stokes, C.R. and Clark, C.D. 2001. Palaeo-ice streams: Quaternary Science Reviews, v. 20, p. 1437–1457.

Strahler, A.N., 1952, Hypsometric (Area–Altitude) analysis of erosional topography: Geological Society of America Bulletin, v. 63, p. 1117–1142, http://dx.doi.org/10.1130/0016-7606(1952)63[1117:HAAOET]2.0.CO;2.

Tague, C., and Grant, G.E., 2004, A geological framework for interpreting the low-flow regimes of Cascade streams, Willamette River Basin, Oregon: Water Resources Research, v. 40, W04303, http://dx.doi.org/10.1029/2003WR002629.

Van Der Beek, P., and Braun, J., 1998, Numerical modelling of landscape evolution on geological time-scales: a parameter analysis and comparison with south-eastern highlands of Australia: Basin Research, v. 10, p. 49–68, http://dx.doi.org/10.1046/j.1365-2117.1998.00056.x.

Walker, J.P., and Willgoose, G.R., 1999, On the effect of digital elevation model accuracy on hydrology and geomorphology: Water Resources Research, v. 35, p. 2259–2268, http://dx.doi.org/10.1029/1999WR900034.

Webster, T.L., 2005, LIDAR validation using GIS: A case study comparison between two LIDAR collection methods: GeoCarto International, v. 20, p. 11–19, http://dx.doi.org/10.1080/10106040508542359.

Webster, T.L., and Dias, G., 2006, An automated GIS procedure for comparing GPS and proximal LIDAR elevations: Computers and Geosciences, v. 32, p. 713–726, http://dx.doi.org/10.1016/j.cageo.2005.08.009.

Webster, T.L., Murphy, J.B., and Gosse, J.C., 2006a, Mapping subtle structures with light detection and ranging (LIDAR): Flow units and phreatomagmatic rootless cones in the North Mountain Basalt, Nova Scotia: Canadian Journal of Earth Sciences, v. 43, p. 157–176, http://dx.doi.org/10.1139/e05-099.

Webster, T.L., Murphy, J.B., Gosse, J.C., and Spooner, I., 2006b, The application of LIDAR-derived digital elevation model analysis to geological mapping: An example from the Fundy Basin, Nova Scotia, Canada: Canadian Journal of Remote Sensing, v. 32, p. 173–193, http://dx.doi.org/10.5589/m06-017.

Wehr, A. and Lohr, U., 1999, Airborne laser scanning—an introduction and overview: ISPRS Journal of Photogrammetry and Remote Sensing, v. 54, p. 68–82, http://dx.doi.org/10.1016/S0924-2716(99)00011-8.

Whipple, K.X., and Tucker, C.E., 2002, Implications of sediment–flux–dependent river incision models for landscape evolution: Journal of Geophysical Research, v. 107, p. 1–20, http://dx.doi.org/10.1029/2000JB000044.

Whipple, K.X., Hancock, G.S., and Anderson, R.S., 2000, River incision into

bedrock: Mechanics and relative efficacy of plucking, abrasion, and cavitation: Geological Society of America Bulletin, v. 112, p. 490–503, http://dx.doi.org/10.1130/0016-7606(2000)112<490:RIIBMA>2.0.CO;2.

Winter, T.C., Harvey, J.W., Franke, O.L., and Alley, W.M., 1998, Ground Water and Surface Water: A Single Resource: United States Geological Survey Circular 1139, p. 79.

Withjack, M.O., Olsen, P.E., and Schlische, R.W., 1995, Tectonic evolution of the Fundy rift basin, Canada: Evidence of extension and shortening during passive margin development: Tectonics, v. 14, p. 390–405, http://dx.doi.org/10.1029/94TC03087.

Wolock, D.M., and Price, C.V., 1994, Effects of digital elevation model map scale and data resolution on a topography– based watershed model: Water Resources Research, v. 30, p. 3041–3052, http://dx.doi.org/10.1029/94WR01971.

Zhang, Xiaoyang, Drake, N.A., Wainwright, J., and Mulligan, M., 1999, Comparison of slope estimates from low resolution DEMs: Scaling issues and a fractal method for their solution: Earth Surface Processes and Landforms, v. 24, p. 763–779, http://dx.doi.org/10.1002/(SICI)1096-9837(199908)24:9<763::AID-ESP9>3.0.CO;2-J.

Zhang, Weihua, and Montgomery, D.R., 1994, Digital elevation model grid size, landscape representation, and hydrological simulations: Water Resources Research, v. 30, p. 1019–1028, http://dx.doi.org/10.1029/93WR03553.

Received April 2012
Accepted as revised July 2013